

CHAPTER 4

The residence time of Focal Adhesion Kinase (FAK) and paxillin at focal adhesions in renal epithelial cells is determined by adhesion size and integrin ligand density

Sylvia Le Dévédec¹, Bart Geverts², Hans de Bont¹, Adriaan B. Houtsmuller^{2,3}, Bob van de Water^{1,3}.

¹*Division of Toxicology, Leiden/Amsterdam Center for Drug Research, Leiden University, Leiden, the Netherlands*

²*Department of Pathology, Josephine Nefkens Institute, Erasmus MC, University Medical Center Rotterdam, the Netherlands*

³A.B.H. and B.v.d.W. contributed equally to this work.

Submitted for publication

ABSTRACT

Focal adhesions (FAs) are specialized membrane associated multi-protein complexes that link the cell to the extra-cellular matrix and enable cell proliferation, survival, and motility. Despite the extensive description of the molecular composition of FAs, the complex regulation of FA dynamics is largely unclear. Here, we describe a new method based on 'half-FRAP' ¹ to measure the diffusion rate, immobile fraction and residence time of individual GFP-tagged focal adhesion-associated proteins using an integrated FLIP (fluorescence loss in photobleaching) - FRAP (fluorescence recovery after photobleaching) technique in combination with Monte-Carlo simulation. We demonstrate that this is a fast and reliable method to elucidate the mobility parameters of any protein localized in all different focal adhesions at the same time in non-migrating epithelial cells. With this method we identified that the focal adhesion proteins FAK and paxillin exist in 3 different states: a fast diffusing cytoplasmic pool, a FA-associated fraction undergoing fast diffusion and a transiently immobile FA-bound fraction with variable residence times. The residence time of both proteins increases with focal adhesion size. However, increasing integrin $\alpha2\beta1$ ligation by modulating surface collagen density increases the time of residence at FAs of FAK but not paxillin. This novel method will enable the rapid analysis of local protein dynamics of many different FA-associated proteins under (patho)physiological conditions.

1. Introduction

Focal adhesions (FA) are transient structures essential in cell adhesion, spreading and migration as well as signaling for cell proliferation and survival²⁻⁶. At FAs the extracellular matrix (ECM), including fibronectin and collagen, is linked to the actin cytoskeleton through clustered integrins and a complex network of cytoskeletal, adapter, and signaling proteins, suggested to exist of at least 150 components, altogether referred to as the 'integrin adhesome'⁶. Steady-state and motile cells can exhibit different types of adhesion such as focal adhesions, fibrillar adhesions or focal complexes⁷. Matrix adhesion sites are highly dynamic which is manifested by their assembly, disassembly and translocation^{8,9}. Continuous remodeling of FAs is critical for example in cell movement and dynamic responses to mechanical forces. Since most components of FAs contain multiple binding sites for other components, the molecular complex can theoretically assemble in numerous ways giving rise to many different supramolecular structures^{7,10}. Further understanding of the dynamic behavior of individual FA components in space and time, will enable a detailed understanding of the mechanism of matrix adhesion dynamics.

The non-receptor tyrosine kinase focal adhesion kinase (FAK) and the adapter protein paxillin are two well-known focal adhesion-associated proteins that are crucial in cell adhesion, migration and invasion¹¹. Both proteins have more than thirty molecular interactions within the 'integrin adhesome' network¹². Upon integrin binding to the ECM, FAK is recruited to FAs and autophosphorylated at tyrosine residue 397 and subsequently phosphorylated by Src at other tyrosine residue, thereby enabling dynamic restructuring of FAs¹³. Paxillin is a structural adaptor protein important in integrin signaling and interacts with FAK as well as various other FA assembly proteins, including vinculin, talin, integrin β 1, Pyk2, c-Src, and Csk^{14,15}. Paxillin localization is at focal adhesions even in the absence of FAK¹⁶. It is phosphorylated on different Ser, Thr and Tyr residues, of which phosphorylation by the FAK/Src complex is essential in cell migration (see review¹⁷). Given the importance of both FAK and paxillin in FA organization and dynamics, further understanding of the molecular behavior of these proteins in individual focal adhesions and the physical-chemical factors that determine the dynamics is important.

Advances in fluorescent probes including genetically encoded fluorescent fusion proteins and imaging technologies have opened the door to studying dynamic cellular processes in living cells. Ideally, for each molecular entity in the cell, one would like to know its concentration, aggregation state, interactions and dynamics in different locations within the cell at different times. Focal adhesion turnover can be quantified using 'apparent' rate constant of focal adhesion proteins, a measurement which integrates the fluorescent intensity in an individual adhesion over time¹¹. However, these apparent rate constants do not reflect the protein's molecular-scale affinity for its binding partners in the adhesion. Over the

years, application of various advanced microscopy techniques contributed to a better understanding in the kinetics of FA proteins. Image correlation spectroscopy (ICS) provided a measure of the coupling between adhesion components and actin¹⁸, as well as fluorescent speckle microscopy was employed to explore interaction between F-actin and FA-associated molecules revealing an apparent flow of FA proteins and actin through FAs¹⁹. Fluorescence Recovery After Photobleaching (FRAP) is an imaging technique that can be used to measure binding and unbinding rate constants of proteins in living cells^{20,21}. FRAP is often used to measure protein exchange dynamics at cell-substrate adhesions but generally report only the half-time of fluorescence recovery ($t_{1/2}$)²²⁻³². A fast and reliable method to evaluate the dynamics of FA proteins in all the FAs in one single cell at the same time and determine more accurately the behavior of these proteins using advanced modeling approaches has not been possible so far.

Here we describe a powerful and reliable photobleaching methodology that provides both spatial and temporal information on protein dynamics in a single cell. We employed simultaneous FLIP (fluorescence loss in photobleaching)-FRAP, also referred to as the 'half-FRAP' technique¹, combined with Monte-Carlo simulation to fit the data and extract protein mobility parameters including as diffusion rate, percentage of bound fraction and residence time¹. We validated the technique by quantifying FAK and paxillin protein mobility parameters in steady-state situation. Although FAK and paxillin have an equal bound fraction at the focal adhesions, FAK resides for a shorter period (60 seconds) at focal adhesions than paxillin (100 seconds). Sorting of FAs by size defined that the residence time for both FAs increases in larger FAs. Furthermore, increasing integrin ligand interaction by modulating collagen density increases the time of residence of FAK but not paxillin. This new method provides new insight in the differential behavior of FAK and paxillin in stable focal adhesion complexes.

2. Materials and methods

2.1 Cell lines

Here we used the porcine renal epithelial cell line LLC-PK1. Cells were maintained in DMEM supplemented with 10% (v/v) FCS and penicillin/streptomycin at 37°C in a humidified atmosphere of 95% air and 5% carbon dioxide. Stable eGFP and eGFP-FAK have been described previously³³. For preparation of stable GFP expressing cell lines, LLC-PK1 cells were transfected with 0.8 µg DNA of pGZ21-paxillin and GFP-actin using Lipofectamine 2000 reagent according to the manufacturer's procedures (Life Technologies, Inc). Stable transfectants were selected using 800 µg/ml G418. Individual clones were picked and maintained in complete medium containing 100 µg/ml G418. Clones were analyzed for paxillin expression using Western blotting and immunofluorescence. For further experiments one representative stable cell lines was used per construct. For

immunofluorescence studies, cells were cultured on collagen coated glass coverslips in 24 well dishes and allowed to adhere overnight in complete culture medium. For live cell microscopy, cells were plated on 35 mm glass coated with either 10 µg/ml collagen (control situation) or 1, 10 or 100 µg/ml collagen (for extra-cellular matrix density experiment) and let stretched in complete medium for overnight. Collagen type 1 from rat tail (Sigma-Aldrich) was stored at 3 mg/ml and diluted to the appropriate concentration for coating in PBS. In all cases, coating was done by incubation for 2 h at 37°C. Coated surfaces were washed three times with PBS and blocked with 1% heat denatured BSA in PBS for 1 h at 37°C.

2.2 Western blot analysis

For Western blot analysis cells were washed twice with PBS and lysed in ice-cold lysis buffer (50 mM HEPES, 150 mM NaCl, 1% (w/v) NP40, 1 mM EDTA pH 7.4) plus inhibitors (2 mM AEBSF, 100 µg/ml aprotinin, 17 µg/ml leupeptin, 1 µg/ml pepstatin, 5 µM fenvalerate, 5 µM BpVphen and 1 µM okadaic acid) for 5 min. After lysis, cells were scraped and centrifuged for 5 min at 4 °C, 14000 rpm. Protein concentrations were determined using Coomassie Protein Assay Reagent using IgG as a standard (Pierce). Equal amounts of protein were separated by SDS-PAGE and transferred to PVDF membrane (Millipore). Blots were blocked with 5% (w/v) BSA in TBS-T (0.15 M NaCl, 50 mM Tris-HCl and 0.05 % (v/v) Tween-20) overnight at 4°C and probed with appropriate primary antibodies for 3h at room temperature as follows: anti-FAK (monoclonal, 1 µg/ml, Transduction Lab.), anti-paxillin (monoclonal, 0.5 µg/ml, Transduction Lab.), anti-GFP (polyclonal, 1 µg/ml, Roche).

2.3 Immunofluorescence

Cells were fixed with 3.7 % formaldehyde for 10 min followed by 3 washes with PBS. After cell permeabilization and blocking with PBS/0.2 % (w/v) Triton X-100/0.5 % (w/v) BSA, pH 7.4 (PTB) cells were stained for P-Tyr397-FAK (BioSource), P-Tyr118-paxillin (BioSource), paxillin (BD Transduction lab) and P-Ser190MLC (Santa Cruz) diluted in TBP. For secondary staining Cy3-labeled goat anti-mouse or anti-rabbit antibodies (Jackson Laboratories) were used. Cells were mounted on glass slides using Aqua-poly-Mount (Polysciences Inc., Warrington, PA). Cells were viewed using a BioRad 2-photon confocal laser scanning microscope and images were processed with Image-Pro® Plus (Version 5.1; Media Cybernetics).

2.4 *Live cell microscopy, Fluorescence recovery after photobleaching (FRAP) and fluorescence loss in photobleaching (FLIP)*

Live-cell microscopy was performed with a Zeiss LSM 510 META confocal laser scanning microscope equipped with a heated (37°C) scan stage and a Plan-Apochromat oil immersion objective (40X, numerical aperture [NA] 1.3, for all FRAP procedures). GFP fluorescence was detected by using the 488-nm line of a fiber-coupled 60-mW argon laser, a dichroic beamsplitter (488/543) and a 510- to 545-bandpass emission filter. All FRAP procedures were performed with the same experimental set-up as for live cell microscopy.

2.4.1 *Strip-FRAP in cytoplasm*

To determine cytoplasmic mobility of GFP, GFP-FAK and GFP-paxillin, a strip 1 μm wide spanning approximately the width of the cytoplasm (without any visible focal adhesion) was photobleached by a short bleach pulse (100 ms) at 100% laser intensity of a 60 mW argon laser at 488 nm. Redistribution of fluorescence within the strip was monitored using 100-ms intervals and low laser intensity to avoid photobleaching by monitoring. Approximately 10 cells were averaged to generate one FRAP curve for a single experiment.

2.4.2 *FRAP on individual focal adhesions*

Spot bleaching was applied to a small area of 0,80 μm^2 covering a single focal adhesion for 1 s at a 50- μW laser intensity. Redistribution of fluorescence was monitored with 100 ms time intervals at low laser intensity starting directly after the bleach pulse. Images were analyzed by using LSM Image software (Zeiss). The relative fluorescence intensity of individual focal adhesion, was calculated at each time interval as follows: $I_{\text{rel}}(t) = (FA_t/FA_0)$, where FA_t is the intensity of the focal adhesion at time point t after bleaching, FA_0 is the average intensity of the focal adhesion before bleaching. Approximately 15 focal adhesions (each in a distinct cell) were averaged to generate one FRAP curve for a single experiment, and the experiment was performed on at least three different days.

2.4.3 *Combined FLIP-FRAP analysis in a single cell*

For simultaneous FRAP and FLIP in a single cell, photobleaching was applied to about half the cell for less than 6 s at high laser intensity. Redistribution of fluorescence was monitored with 6 s time intervals. We processed the different time lapse movies using Image Pro software using in house written macro where focal adhesions were segmented based on intensity. Fluorescence intensity values over the time for each focal adhesion were exported into Excel together with FA morphologic parameters (size, elongation, area, localization). The difference between relative fluorescence intensities of bleached (FRAP) and unbleached

(FLIP) focal adhesion was calculated as $I_{rel}(t) = \frac{([FA_t\text{-background}]/[FA_0\text{-background}])_{\text{unbleached}} - ([FA_t\text{-background}]/[FA_0\text{-background}])_{\text{bleached}}}{([FA_t\text{-background}]/[FA_0\text{-background}])_{\text{unbleached}}}$ and normalized to the first data point after bleaching. Approximately 5 cells with more than 50 focal adhesions per cell were averaged to generate FRAP and FLIP curves for a single experiment, and the data shown were performed on at least three different days.

2.5 FRAP analysis

For analysis of FRAP data, FRAP curves were normalized to prebleach values and the best fitting curve (least squares) was picked from a large set of computer simulated FRAP curves in which three parameters representing mobility properties were varied: diffusion rate (ranging from 1 to 25 $\mu\text{m}^2/\text{s}$), immobile fraction (0, 10, 20, 30, 40, 50 %) and time spent in immobile state, ranging from 10, 20, 30, 40s to ∞ s. Monte Carlo computer simulations used to generate FLIP and FRAP curves were based on a cell model of diffusion (ellipsoid volume representing the cytoplasm of the cell which includes another smaller ellipsoid volume representing the nucleus), and simple binding kinetics representing binding to immobile elements in the cell, representing focal adhesions (Fig. 3). Simulations were performed at unit time steps corresponding to the experimental sample rate of 5 s. Diffusion was simulated by each step deriving novel positions $M(x+dx, y+dy, z+dz)$ for all mobile molecules $M(x, y, z)$, where $dx = G(r_1)$, $dy = G(r_2)$ and $dz = G(r_3)$, r_i is a random number ($0 \leq r_i \leq 1$) chosen from a uniform distribution, and $G(r_i)$ is an inverse cumulative Gaussian distribution with $\mu = 0$ and $\sigma^2 = 2Dt$, where D is the diffusion coefficient and t is time measured in unit time steps. Immobilisation was based on simple binding kinetics described by: $k_{on}/k_{off} = F_{imm}/(1 - F_{imm})$, where F_{imm} is the relative number of immobile molecules. The chance for each particle to become immobilized per unit time (representing focal adhesion-binding) was defined as $P_{immobilise} = k_{on} = k_{off} \cdot F_{imm}/(1 - F_{imm})$, where $k_{off} = 1/t_{imm}$, and t_{imm} is the average time spent in immobile complexes measured in unit time steps; the chance to release was $P_{mobilise} = k_{off} = 1/t_{imm}$. The FRAP procedure was simulated on the basis of an experimentally derived three-dimensional laser intensity profile providing a chance based on three-dimensional position for each molecule to get bleached during simulation of the bleach pulse.

2.6 Statistical Analysis

Student's t test was used to determine significant differences between two means ($p < 0.05$).

3. Results

3.1 Mobility of GFP-FAK and GFP-paxillin in the cytosol and at focal adhesions of living cell

To study the dynamics of both focal adhesion associated proteins we used the renal epithelial cell line LLC-PK1, a well characterized cell line adherently growing on rigid planar substrate characterized by prominent matrix adhesions that are abundant and quite large in shape³³. To study the behavior of FAK and paxillin in matrix adhesions, we generated LLC-PK1 cell lines ectopically expressing either GFP-FAK and GFP-paxillin, in which the expression was present in similar amount as the endogenous counterparts and predominantly located at focal adhesions in living cells (Fig.S1A-C). LLC-PK1 cells expressing GFP or GFP-actin were used as controls in some of the experiments. Importantly, live cell imaging demonstrated that GFP-FAK and GFP-paxillin containing FAs remain stable over a time period of 15 min (Fig.S1D and movie M1 and M2), allowing a reliable timescale of 5 minutes to study protein dynamics using FRAP technology.

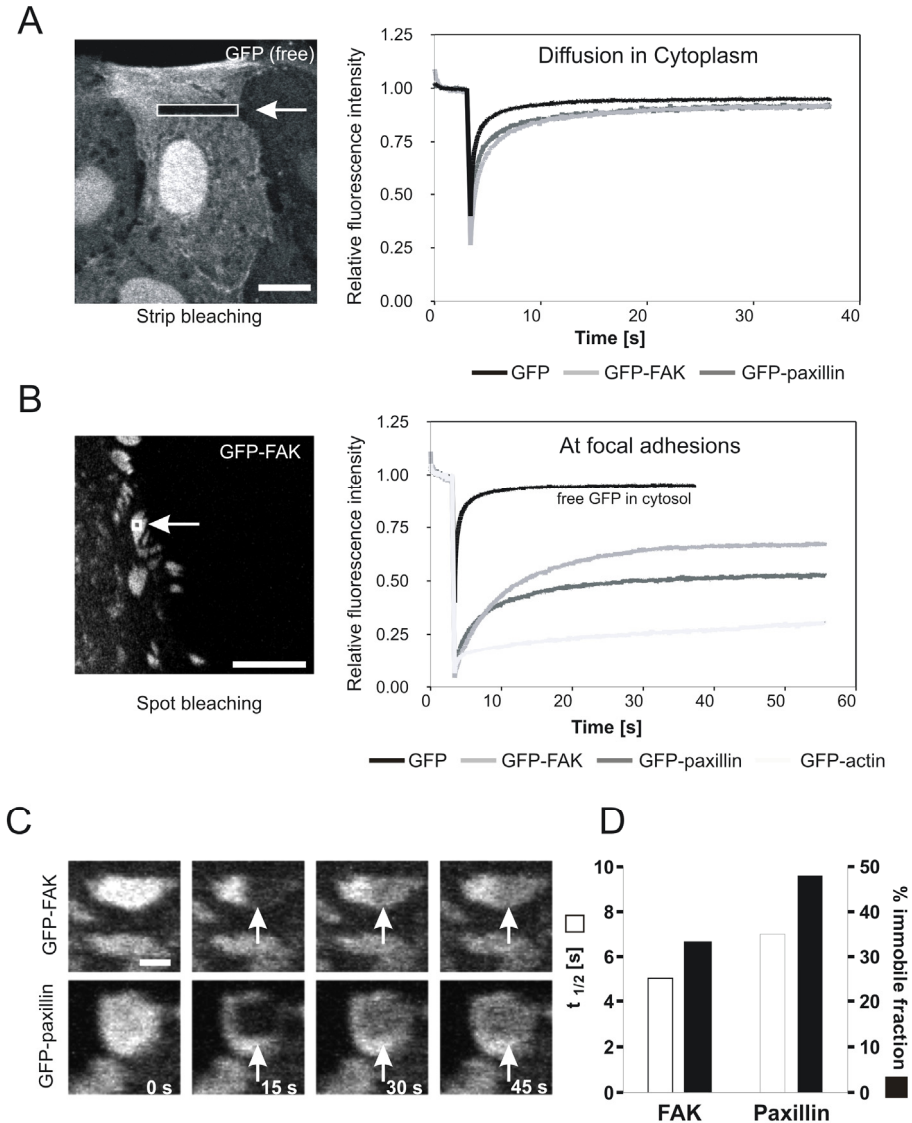


Figure 1: FRAP analysis of cytosolic and focal adhesion-associated GFP-FAK and GFP-paxillin. (A) Quantitative analysis of fluorescence redistribution of GFP (n=20), GFP-FAK (n=30) and GFP-paxillin (n=30) after strip bleaching in the cytoplasm. A small strip of 1,8 μm wide spanning was photobleached (white box). Scale bar, 20 μm . Note that the fluorescent intensity in the strip does not recover to prebleach levels (set to one) because a fraction of the molecules is permanently bleached. (B) Quantitative analysis of fluorescence redistribution of GFP (n=20), GFP-FAK (n=45), GFP-paxillin (n=45) and GFP-actin (n=45) after spot bleaching in the focal adhesions. A small region of 1 μm^2 covering a single focal adhesion was photobleached (white box). Scale bar, 10 μm . (C) Examples of spot bleaching (arrowhead) on a single GFP-FAK and GFP-paxillin expressing focal adhesion. Images were acquired before bleaching and at 5 s intervals after bleaching. Scale bar, 1 μm . (D) Average half-time for fluorescence redistribution after photobleaching ($t_{1/2}$, s) and % immobile fraction for GFP-FAK and GFP-paxillin.

First we investigated whether GFP-FAK and GFP-paxillin are bound to subcytoplasmic structures/protein complexes or are moving freely throughout the cells. We measured the GFP-FAK and GFP-paxillin cytoplasmic mobilities by applying strip FRAP. Cytoplasmic diffusion was assessed in regions in between focal adhesions. The rate of redistribution of fluorescence in the bleached strip is a measure for the diffusion rate of the tagged protein. Analysis of the FRAP data revealed that the majority of GFP-FAK and GFP-paxillin molecules were freely mobile in the cytoplasm and show similar diffusion rate, but slower than GFP only (Fig. 1A). Next, association of GFP-FAK and GFP-paxillin at focal adhesions was assessed by spot bleaching of a small region of $0.8 \mu\text{m}^2$ covering a single focal adhesion and subsequent quantitative analysis of fluorescence redistribution specifically at the bleached focal adhesion (Fig. 1B and C). FRAP analysis indicated fast but different binding kinetics of FAK and paxillin at focal adhesions: for FAK a $t_{1/2} = 5\text{s}$ and a 33% immobile fraction was determined, while for paxillin a $t_{1/2} = 7\text{s}$ and a 50% immobile fraction was observed. This indicates that more than 50% of the signal of both proteins is due to diffusing molecules and that immobile fractions recover in a much longer period than 60s illustrating the dynamic interaction of paxillin and FAK with focal adhesion in LLC-PK1 cells. This is in sharp contrast to the dynamics of GFP-actin, which shows hardly any redistribution even after 10 min (Fig. 1B). Importantly, GFP-FAK and GFP-paxillin redistribution at focal adhesions was slower compared to their apparent diffusion rate in the cytoplasm, indicating that the rate of recruitment of these molecules to focal adhesions is not diffusion limited. No difference in FRAP recovery curves in the cytoplasm was measured at 25°C , (Fig. S2), indicating that FAK moves by diffusion²⁰. Nonetheless, the FRAP recovery curve of FAK was slower at 25°C which could indicate that FAK is involved in some temperature dependent process in which it is a bit shorter immobilized at lower temperature at focal adhesions.

3.2 Half-FRAP an adapted bleaching approach for studying focal adhesions

The spot bleaching approach is useful to study focal adhesion associated protein kinetics, but does not allow the analysis of behavior of proteins in all focal adhesions within one cell. Therefore we performed complementary simultaneous FLIP (Fluorescence Loss in Photobleaching)-FRAP bleaching assays, (half-FRAP), in combination with Monte Carlo simulation, is currently used to study protein dynamics in the nucleus in whole cells^{1,34-36}. We applied this approach to study the dynamics of all focal adhesions in single cells by a direct comparison of bleached (FRAP) and unbleached (FLIP) focal adhesions, thus avoiding potential errors due to loss of fluorescence by the bleached pulse and by monitor bleaching. We first performed 'half-FRAP' in GFP-FAK cells. In less than 6s half of the cell was bleached. Fluorescence recovery in the bleached area (FRAP) and loss in fluorescence in the unbleached area (FLIP) was monitored over a time period of 5 min (every 6 seconds). Next, redistribution of fluorescence was analyzed at focal

adhesions and in the cytoplasm of the GFP-FAK cells (Fig. 2A). Regions without any focal adhesions were selected in the cell to determine the diffusion coefficient. Focal adhesions localized at the cell periphery (peripheral FAs) were all selected by image segmentation for further analysis (Fig. S3 for an example of analysis). For correct image processing, we defined 6 regions over the entire cell area from the bleach front (three in the direction of the FRAP area, and three in the direction of the FLIP area). Each region had a width of 50 pixels. The first regions from the front were either defined as FRAP 0-50 or FLIP 0-50 (Fig. 2A). We averaged FLIP and FRAP curves of individual focal adhesion located in corresponding regions (Fig. 2B). The difference in relative fluorescent intensity between the FLIP and the FRAP region was then plotted to allow comparison (Fig. 2C). Typically, in one time-lapse series we could analyze more than 50 focal adhesions in one cell from which different parameters including fluorescence intensity over time, shape, perimeter, area and localization in the cell were determined. It can be observed that the FLIP-FRAP curves decay faster in the region close to the edge of the bleached region (Fig. 2C). Furthermore there is clear difference in protein dynamics when the protein was localized in the cytoplasm compared to focal adhesions demonstrating the binding activity of paxillin at focal adhesion sites. Similar experiments and analyses were performed with GFP-paxillin and GFP expressing cells. (Fig. S4). Altogether these data indicate that the mobility of freely mobile paxillin are similar to that of FAK. In contrast, FAK turns over faster than paxillin at focal adhesion sites.

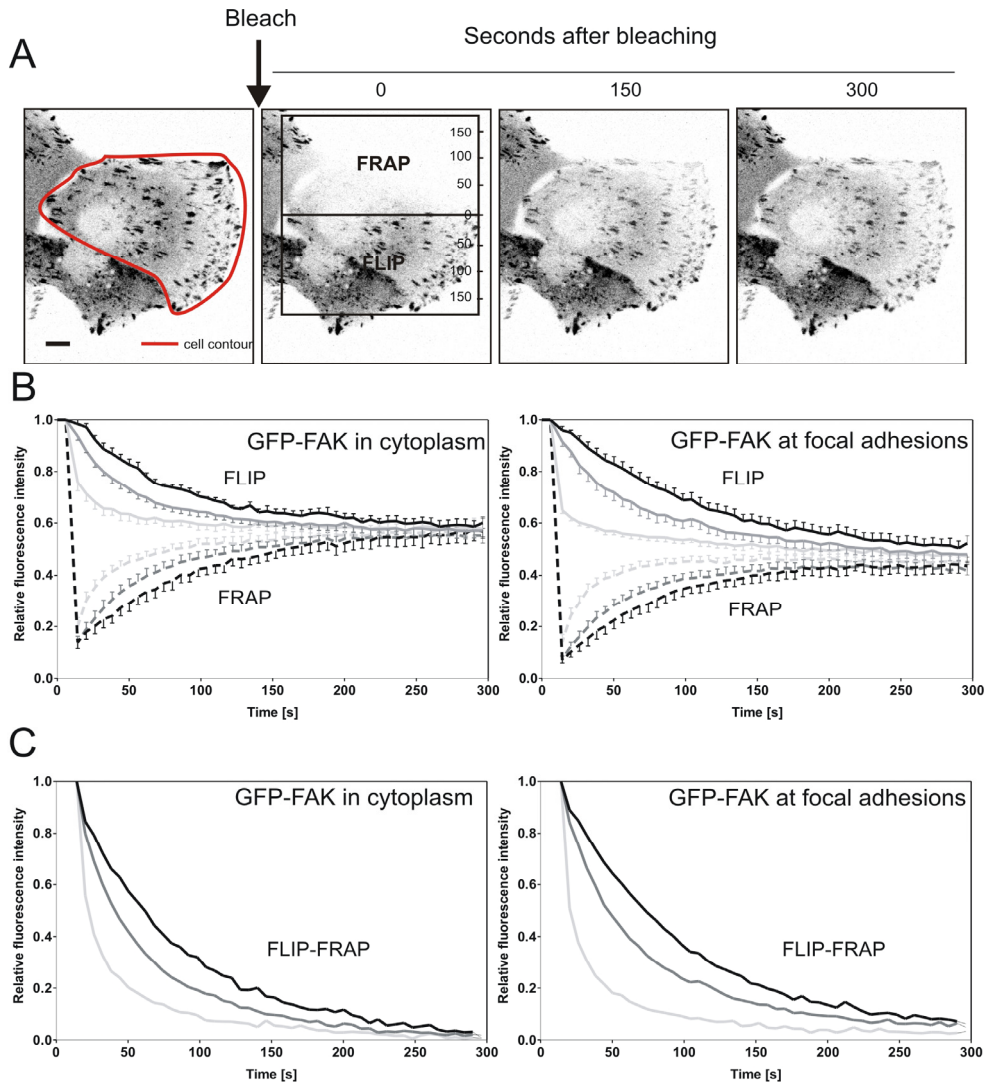


Figure 2: Simultaneous FLIP-FRAP (=half-FRAP) of focal-adhesion bound GFP-FAK. (A) FLIP-FRAP on living LLC-PK1 cells expressing GFP-FAK. Cells are photobleached over a region covering about one half of the cell (indicated by black boxes). The images were acquired before bleaching and at 6-s intervals after bleaching. Scale bar is 10 μm . (B) Quantitative analysis of redistribution of GFP-FAK in the cytoplasm and at focal adhesion separately in bleached and unbleached (and in the 3 different regions) half of the cell. Values are means \pm SEM from at least 25 cells. (C) Differences in GFP intensity in bleached and unbleached parts of the cell (=FLIP-FRAP) calculated from the data shown in panel B.

3.3 FAK and paxillin diffuse similarly in the cytoplasm but associate with focal adhesion in two distinct kinetic pools

To further analyze the experimental data and apply Monte Carlo simulation, we first required a cell model that represents the LLC-PK1 cells. Therefore, we obtained several z-scans of living LLC-PK1 expressing different GFP-tagged proteins cells (Fig. 3A) to generate a general schematic cell model which had an average length of $\sim 60 \mu\text{m}$, width of $\sim 40 \mu\text{m}$ and height of $\sim 30 \mu\text{m}$ (Fig. 3B). A cell model based on one ellipsoid was designed which represents the cytoplasm and an empty ball representing the nucleus, representing lack of GFP-paxillin and GFP-FAK staining in the nucleus (see e.g. Fig. S1B). We also assigned a number of objects as focal adhesions located in the 6 different regions (FRAP and FLIP at 0-50, 50-100, 100-150 pixels) at the bottom of the cell (Fig. 3C).

This LLC-PK1 cell model was used together with Monte Carlo computer simulation to fit the experimental half-FRAP data obtained either in the cytoplasm or at the focal adhesions. The diffusion coefficients were determined by least square fitting to curves obtained from computer simulations in which diffusion, association and dissociation rates to and from focal adhesions were varied. The GFP-FAK and GFP-paxillin data fitted best to a D_{eff} of approximately $\pm 4 \mu\text{m}^2/\text{s}$ (Fig. 3E). Free cytoplasmic GFP showed a faster redistribution with a D_{eff} of $15 \mu\text{m}^2/\text{s}$ (D_{eff} for example in human fibroblast is $18 \mu\text{m}^2/\text{s}$; ¹), clearly higher than that of GFP-FAK and GFP-paxillin which revealed their bound state also in the cytoplasm. We calculated the ratio between total focal adhesion and total cytoplasmic fluorescence. Because GFP fluorescence intensity is proportional to GFP-FAK or GFP-paxillin concentration, this ratio should give a good estimate of the fraction of GFP-FAK and GFP-paxillin bound to the focal adhesions. The average intensity for GFP-FAK and GFP-paxillin at the focal adhesions was 2.7 times higher than in the cytoplasm indicating that FAK and paxillin are both bound for approximately 73% to the focal adhesions, in accord with previous measurements of immobile fraction of adhesion proteins (74%; ¹⁸). Simultaneous FLIP-FRAP analysis indicated that GFP-FAK is almost completely redistributed over bleached and unbleached focal adhesions within 5 minutes after bleaching (Fig. 2B and C). In contrast, GFP-paxillin redistribution is not complete within this time interval (Fig. S4B). Computer simulation of the experimental data indicated rapid exchange of FAK at focal adhesion in two fractions: one fast component which diffuses at $\pm 4 \mu\text{m}^2/\text{s}$ and one slower component showing a residence time of $\sim 60 \text{ s}$ at the focal adhesions. The binding kinetics of GFP-paxillin were characterized by a secondary slow component (residence time of $\sim 100\text{s}$), in addition to a rapidly exchanging fraction with an association constant remarkably similar to that of FAK (Fig. 3F). These data show that the dynamics of the two well known partners FAK and paxillin are actually different from each other.

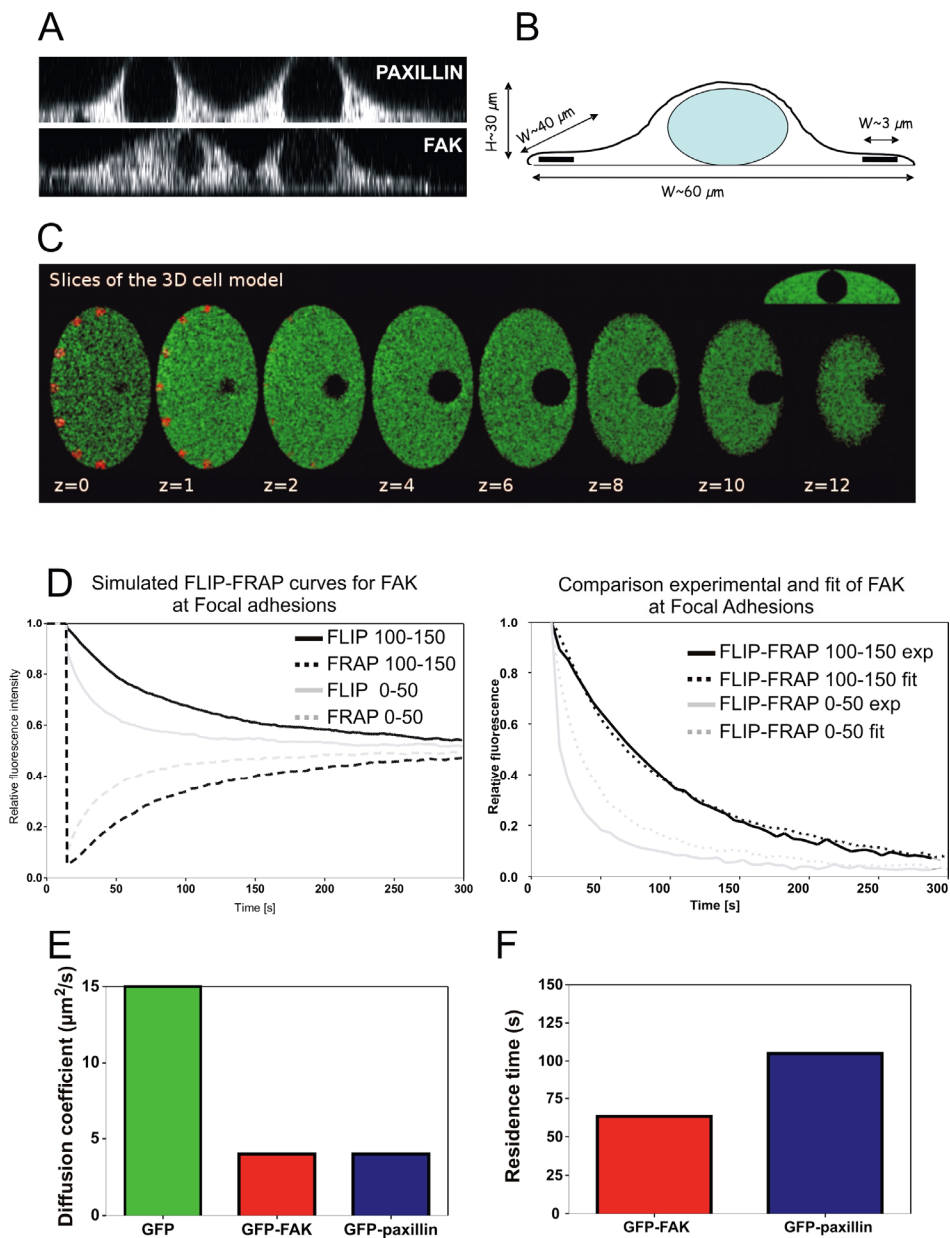


Figure 3: 3D cell model to use Monte-Carlo simulation. (A) Z-scan projection of LLC-PK1 cells expressing GFP-paxillin and GFP-paxillin. Scale bar, μm . (B) Schematic view of a LLC-PK1 cell in steady-state. (C) 3D cell model used for Monte-Carlo simulation. One ellipsoid represents the cytoplasm and an empty ball represents the nucleus. The red structures are the objects that represent focal adhesions located in the different FLIP-FRAP regions. , the green particules are the GFP-molecules. (D) Fitting analysis of experimental data from FLIP-FRAP curves representing regions 0-50 and 100-150 for FA-associated paxillin and FAK. (E). Mobility parameters (diffusion coefficient and residence time) of FAK and paxillin obtained after Monte-Carlo simulation and data fitting.

3.4 Increased residence time of FAK and paxillin is correlated with focal adhesion size

A very attractive advantage of our half-FRAP approach is the collection of multiparametric data on every focal adhesion in each bleached cell. Hence, we can sort the adhesions according to their size, elongation, area or distribution and extract for each adhesion type the mobility parameters of the investigated protein. We analyzed whether the mobility of FAK and paxillin is dependent on the FA size. We sorted all FA based on size (Fig. 4A); GFP-FAK and GFP-paxillin cells showed a similar number of focal adhesions per cell (Fig. 4B). We categorized the focal adhesions in 3 surface areas: 0 to 1 μm^2 , 1 to 3 μm^2 , 3 to 15 μm^2 . Each cell possessed ~ 50 focal adhesions of the smallest area and less than 10 focal adhesion of the biggest area. No linear relationship was observed between adhesion size and molecular density: the mean GFP intensity only slightly increased with focal adhesion size for both FAK and paxillin cells (Fig. 4C). Then we plotted the FLIP-FRAP curves (Fig. 4D) of both focal adhesion proteins according to the focal adhesion area. The data indicate that the redistribution of both GFP-FAK and GFP-paxillin are dependent on focal adhesion size. Finally, the FLIP-FRAP curves were used for Monte Carlo simulation. The residence time of FAK as well as paxillin in large focal adhesions was two-fold higher compared to the smaller adhesion (Fig. 4E). The residence time of paxillin was consistently higher than FAK at all adhesion areas (Fig 4E). These data clearly indicate that the larger focal adhesions are the stronger the association of FAK and paxillin with these focal adhesions is.

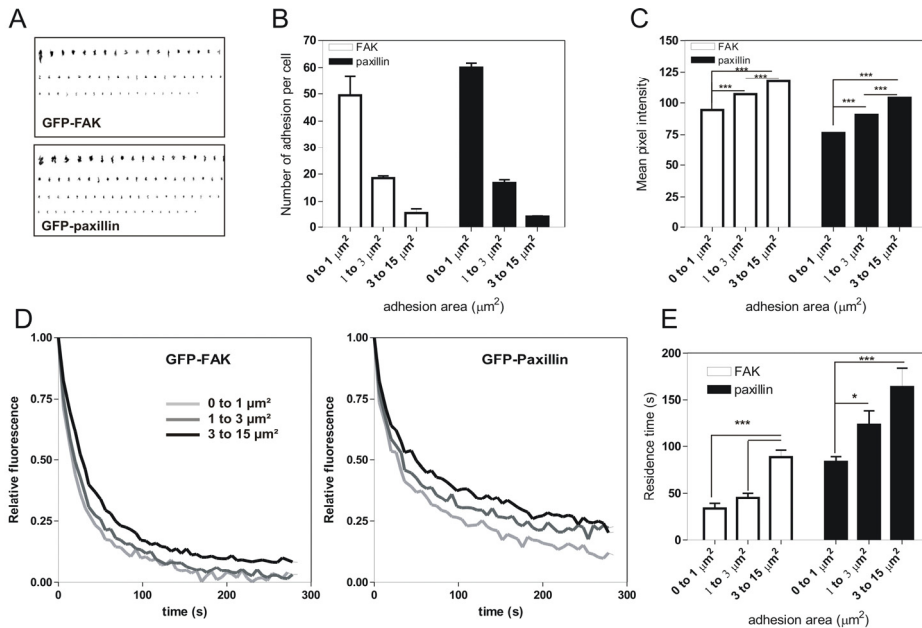


Figure 4: Focal adhesion size is a function of protein density and residence time. (A) Examples of matrix adhesion variety in cells expressing GFP-FAK and GFP-paxillin. After image segmentation based on intensity threshold, objects such as focal adhesions can be displayed according to the size using Image-Pro-Plus software. (B) Plot shows the number of adhesions per cell versus adhesion size (μm^2). Values are means \pm SEM. No significant difference between FAK and paxillin. (C) Plot shows the mean pixel intensity versus adhesion size which is equivalent to the adhesion density. Values are means \pm SEM and are all significantly different from each other. Size versus adhesion density ($p < 0.0001$) and FAK versus paxillin ($p < 0.0001$). (D) FLIP-FRAP curves of GFP-FAK and GFP-paxillin sorted according to the adhesion area. (E) Plot shows residence time of both FAK and paxillin versus adhesion area (μm^2).

3.5 Rapid FAK and paxillin dissociation from focal adhesions correlates with adhesion strength

The number of focal adhesions, their size, distribution and dynamics is defined by ECM composition and density³⁷, thereby determining³⁸ cell migration. Here we next determined whether ECM density affects the residence time of FAK and paxillin at focal adhesions^{37,39}. GFP-FAK- and GFP-paxillin-LLC-PK1 cells were plated on different collagen densities (1, 10, 100 $\mu\text{g}/\text{ml}$). At 100 $\mu\text{g}/\text{ml}$ collagen LLC-PK1 cells did not fully spread compared to the lowest 1 and 10 $\mu\text{g}/\text{ml}$ collagen (Fig. S5A). Moreover, under these conditions, cells had only peripheral FAs that were large in size and always associated with thick peripheral F-actin bundles that also were positive for P-Ser19-MLC, indicative for a contractile phenotype⁴⁰ (Fig. S5B-C). Next, we performed half-FRAP experiments for both GFP-FAK and GFP-paxillin cells at 1, 10 and 100 $\mu\text{g}/\text{ml}$ collagen concentrations. For all conditions we quantified all focal adhesions in GFP-paxillin and GFP-FAK

cells. At high collagen concentration, the number of small focal adhesions decreased while more large focal adhesions were observed (Fig. 5A). The molecular density, which is higher in GFP-FAK cells than in GFP-paxillin cells, increased with focal adhesion size and also with the collagen concentration (Fig. 5B). Finally, we fitted the FLIP-FRAP curves and focused on the focal adhesion population at a 100-150 pixel distance from the bleach front. (Fig. 5C and D). Monte Carlo simulation revealed that the residence time of paxillin was hardly affected by ECM substrate density and remained around 120 sec. The residence time of FAK at focal adhesions increased with higher collagen density by two-fold (Fig. 5D). This leads to a model in which intermediate adhesion strength correlates with a shorter residence time of both FAK and paxillin (Fig.6)⁴¹. Together, these data indicate that adhesion strength controls focal adhesion proteins turnover.

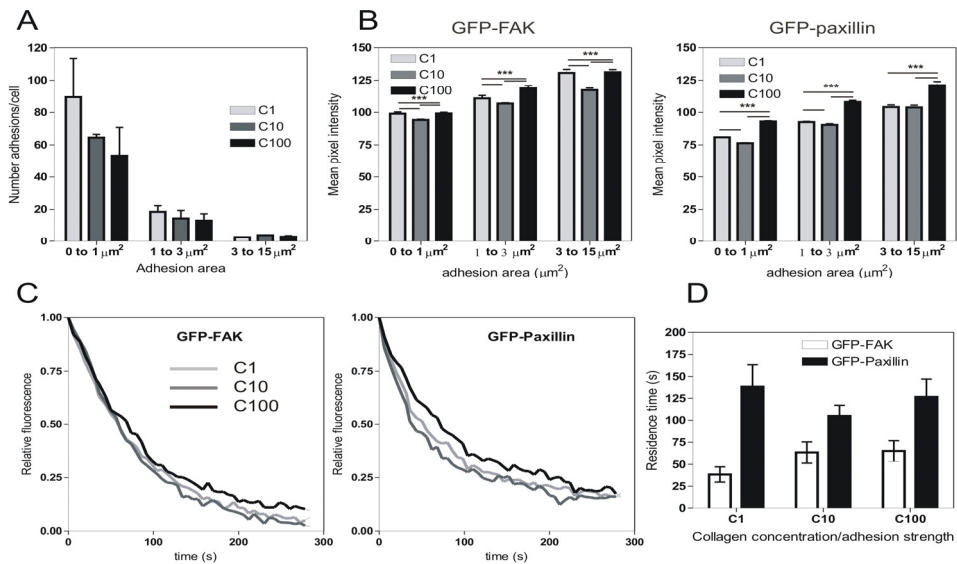


Figure 5: Shortest residence time of FAK and paxillin correlates with intermediate adhesion strength. (A) Plot shows the number of adhesions per cell plated on low, medium and high CN versus adhesion size (μm^2). (B) Plots show adhesion density on low, medium and high CN versus adhesion size for GFP-FAK and GFP-paxillin respectively. Values are means \pm SEM and are all significantly different from each other. Size versus adhesion density ($p < 0.0001$) and FAK versus paxillin ($p < 0.0001$). (C) Examples of FLIP-FRAP curves of the region 100-150 of GFP-FAK and GFP-paxillin on low, medium and high CN. (D) Plot shows residence time of both FAK and paxillin versus collagen concentration. Values are means \pm SEM. No significant difference between FAK and paxillin.

4. Discussion

Understanding the molecular mechanisms that orchestrate the dynamics of focal adhesions is necessary to improve our insight in the fundamental process of cell migration. In the present study, we have used a fast and reliable adapted photobleaching methodology (half-FRAP) combined with Monte-Carlo simulation to determine the spatial and temporal behavior of individual focal adhesion components at cell matrix adhesion complexes within living cells. We applied this technique to determine the dynamic behavior of FAK and paxillin, two central focal adhesion proteins, in the cytoplasm and within focal adhesions in stationary epithelial cells plated on collagen and on increasing adhesion strength. Our data indicate that: i) FAK and paxillin exist in 2 different states: a fast diffusing cytoplasmic pool, and a transiently immobile FA-bound fraction with variable residence times; ii) residence time of both FA proteins increase with increasing size; and iii) adhesion strength increases by modulating ECM ligand density increases the time of residence at FAs of FAK but not paxillin. We propose a model where both clustering and integrin-mediated adhesion strength of cell matrix adhesion complexes is correlated with the residence time of FAK and paxillin at these sites (Fig. 6).

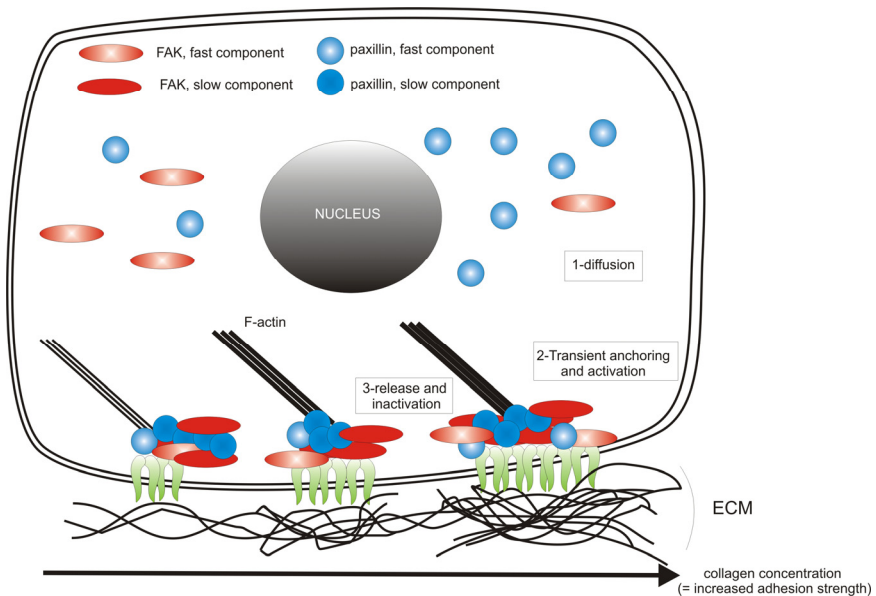


Figure 6: Model for FAK and paxillin dynamics in epithelial cells in steady-state. Non phosphorylated FAK and paxillin molecules (light red and blue) are free to diffuse in the cytoplasm. When transiently anchored to the focal adhesions FAK and paxillin will get phosphorylated (dark red and blue) and remain in the focal adhesions for a certain period of time depending on the focal adhesion size and the ECM density.

We established a novel strategy to fast and accurately determine the residence time of adhesion-associated proteins. So far FRAP has extensively been used to study adhesion protein kinetics^{22,24,27-29,42}. Most studies report the $t_{1/2}$ value which represents a combination of protein diffusion, binding and unbinding kinetics. Likewise, measured change in $t_{1/2}$ can arise from variations in one or more of these parameters. Because of potential diffusion limitations, $t_{1/2}$ is not an optimal metric for comparison of intrinsic binding properties of proteins. Recently, a new approach based on FRAP and the use of mathematical models has been used to measure the dissociation rate constant k_{off} of GFP-vinculin and GFP-zyxin^{29,32,43,44}. Our half-FRAP/Monte Carlo simulation approach determines similar protein mobility parameters but it does that not only with few focal adhesions bleached individually but on all the focal adhesions of a cell. This provides a mapping of protein parameters according to the focal adhesion size and distribution over the cell body.

We determined that GFP-FAK and GFP-paxillin are recruited to focal adhesions with a diffusion coefficient of $\pm 4 \mu\text{m}^2/\text{s}$. So diffusion leads to the possibility to get to focal adhesion in a random way, no directed movement is observed, and that 'recruitment', is a result of affinity. This result is similar to the value determined also by FRAP of paxillin-YFP in HeLa cells³². Also in CHOK1 cells, cytosolic GFP-paxillin had a diffusion coefficient in the same order of magnitude of $D = 8.3 \mu\text{m}^2/\text{s}$, as determined by raster image correlation spectroscopy (RICS)⁴⁵. Since both GFP-FAK and GFP-paxillin show very close similarity in the D_{eff} , but clearly larger than GFP, is indicative that FAK and paxillin might move together in the cytoplasm in larger complexes although both proteins differ in their residence time meaning that they do not release together from the focal adhesions.

Our Monte Carlo simulation shows that FAK and paxillin are transiently immobilized to the focal adhesions with residence time of respectively 60s and 100s. This is in the same order of magnitude as observed in capillary endothelial cells using FRAP and mathematical modelling (~10 seconds for FAK and ~26 seconds for paxillin⁴⁴). As the focal adhesions grow in size and molecular complexity, FAK and paxillin show slower kinetic explained by a longer residence time. Despite the fact that FAK and paxillin both localize at focal adhesions, they clearly differ in their behaviour. This can be explained by the differences in the set of focal adhesion binding partners of both proteins that are related to¹². Thus, while paxillin has strong interaction with various structural components in focal adhesions (more than 30), including FAK, Src, talin, ILK, Crk, PAK, tubulin and actin, FAK rather associates with signalling intermediates as well as some adapter proteins such as FAK, Src, p190Gap, calpain and others. Also, the binding property and kinase activity of FAK control its dynamics since FAK lacking its kinase domain (FAT) shows increased exchange between FAs and cytosol (supplemental data 2B, ^{27,42}).

Our data indicate that adhesion strength affects FAK and paxillin transient immobilization in focal adhesions. In our model system the degree of ECM ligand density seems to determine intracellular tension. Thus, P-Ser19-MLC levels, indicative for actin/myosin stress fiber tensions, were higher in LLC-PK1 plated on high ECM density (Fig. 6). Several studies demonstrate that tension is an important determinant for adhesion size and molecular (phospho-) protein composition of FAs. In human foreskin fibroblasts, the amount of tension generated by a focal adhesion correlates with focal adhesion size and with the local accumulation of the focal adhesion adaptor protein GFP-vinculin⁴⁶. Moreover, cytoskeletal stiffness mediates increase in focal adhesion size and density along with changes in their molecular composition⁴⁷, while localization and turnover of zyxin was tension-dependent^{48,49}.

We show that in LLC-PK1 cells FAK and paxillin exist in 3 different states: a fast diffusing cytoplasmic pool, a FA-associated fraction undergoing fast diffusion and a transiently immobile FA-bound fraction showing variable residence times. Using a spot bleaching approach in combination with mathematical modeling, Wolfensen and colleagues demonstrated even four distinct dynamic population of paxillin-YFP in the HeLa-cells: a fast diffusing cytoplasmic population, a second population with intermediate redistribution on a 3 s timescale, a third population with slow redistribution and a fourth which is immobile³². We were not able to distinguish between the fast and intermediate redistribution paxillin populations, which could be due to the different type of cells used and our half-FRAP methodology. Nevertheless, future novel algorithms in the Monte Carlo simulation may allow the discrimination of alternative subpopulations with slightly different kinetics.

In conclusion, our combined FLIP-FRAP approach allows us to analyze all focal adhesions in individual cells with respect to type, size and distribution which we can be correlated to the protein dynamics. With this half-FRAP procedure, we are able to generate detailed cellular maps of focal adhesion protein dynamics including: i) motility parameters of cytosolic and FA-associated proteins, ii) proteins dynamics in relation to their spatial localization and iii) changes in protein dynamics following perturbations. The practicality and general applicability of this technique in a wide variety of settings should prove useful in further characterizing the regulation of matrix adhesions under different biological settings. A quantitative mapping of the residence times of all FA proteins in the entire cell according to its localization (ventral/dorsal), size and type remains a fundamental next challenge. We think our half-FRAP is a suitable approach to reach this goal.

Acknowledgments

We thank the imaging members of the Division Toxicology for helpful suggestions and the IOC imaging center at Erasmus Rotterdam technical support. This work

was supported by the Dutch Cancer Society (grants UL 2006-3538 and UL 2007-3860) and the EU FP7 Metafight project (Grant agreement no.201862).

SUPPLEMENTAL DATA:

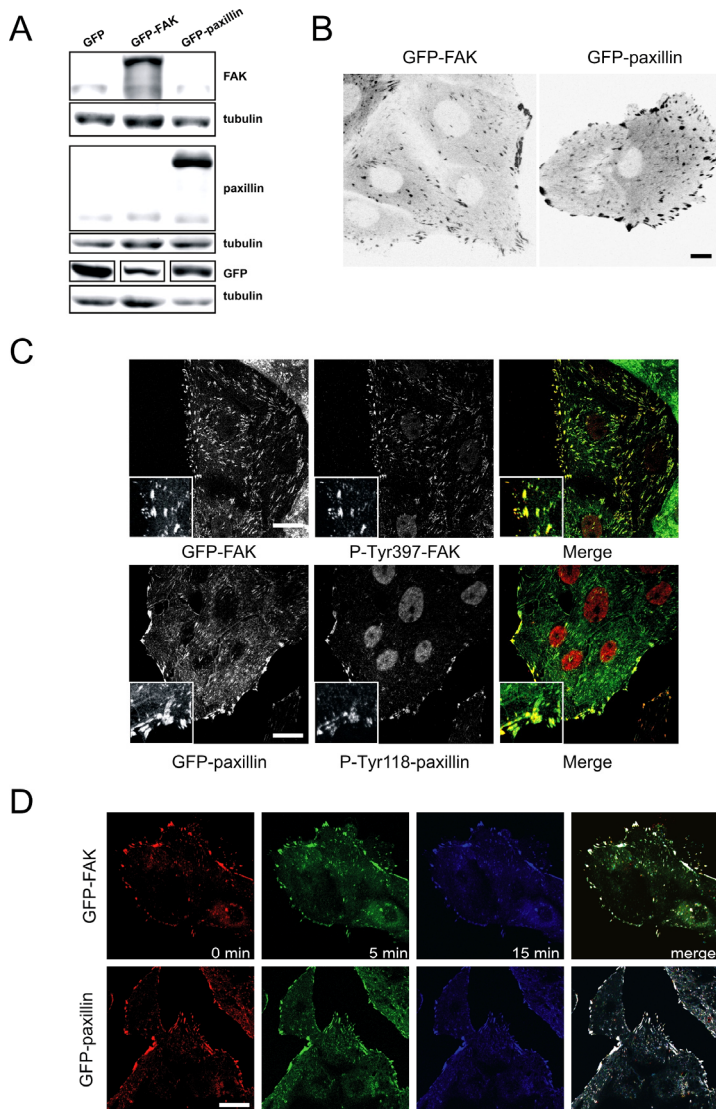


Figure S1: Expression levels, localization and turnover of GFP-FAK and GFP-paxillin. (A) Immunoblot of whole cell extracts of LLC-PK1 cells with stable expression of GFP (lane 1), GFP-FAK (lane 2) and GFP-paxillin (lane 3) probed with anti-FAK, anti-paxillin and anti-GFP antibodies. (B) Confocal images of living GFP-FAK and GFP-paxillin expressing cells. Scale bar, 10 μ m. (C) P-tyr397 FAK and P-tyr118 paxillin staining in respectively GFP-FAK and GFP-paxillin expressing cells. Scale bar, μ m. (D) Time-lapse of GFP-FAK and paxillin expressing cells for 15 min. Note the stability of the focal adhesions over the period of time of 15 min in the merge picture. Scale bar is 10 μ m.

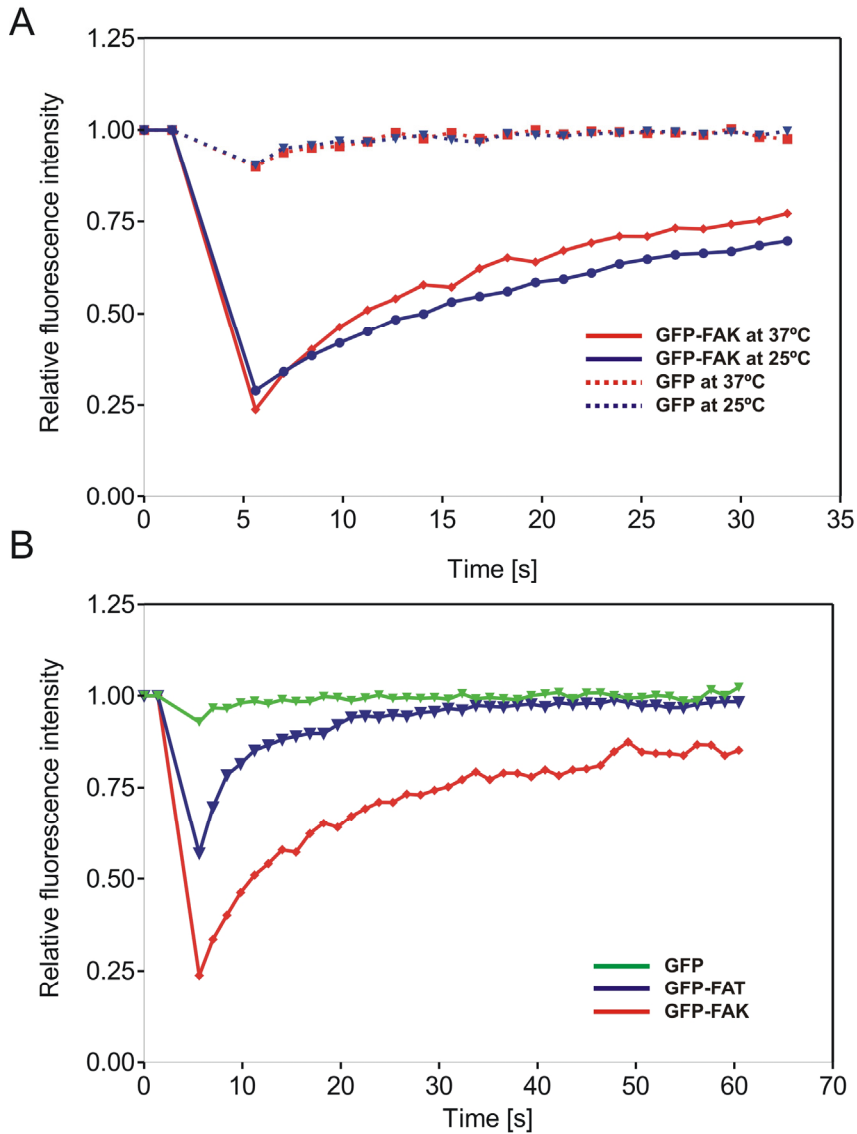


Figure S2: GFP-FAK is freely mobile and move by diffusion and its dynamics depends on binding domains. (A) Quantitative analysis of redistribution of GFP and GFP-FAK at individual bleached focal adhesion in living cells maintained at 37 °C (red line) and 25 °C (blue line). (B) Quantitative analysis of redistribution of GFP (green), GFP-FAK (red) and GFP-FAT (blue) at individual bleached focal adhesion in living cells maintained at 37 °C.

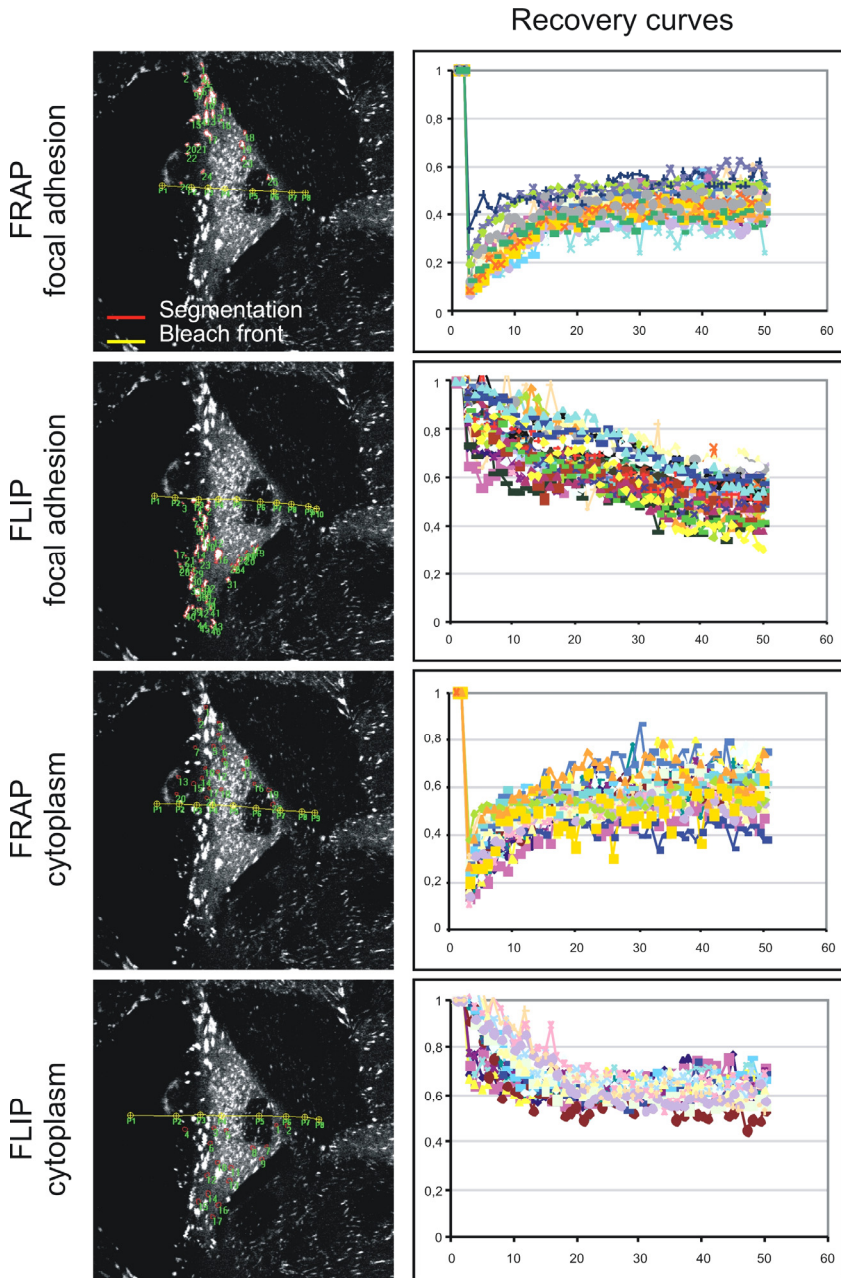


Figure S3: Example of data analysis of a FRAP experiment performed on a GFP-paxillin LLC-PK1 cell. Individual FRAP and FLIP curves for each focal adhesions obtained after threshold segmentation and for the cytoplasm.

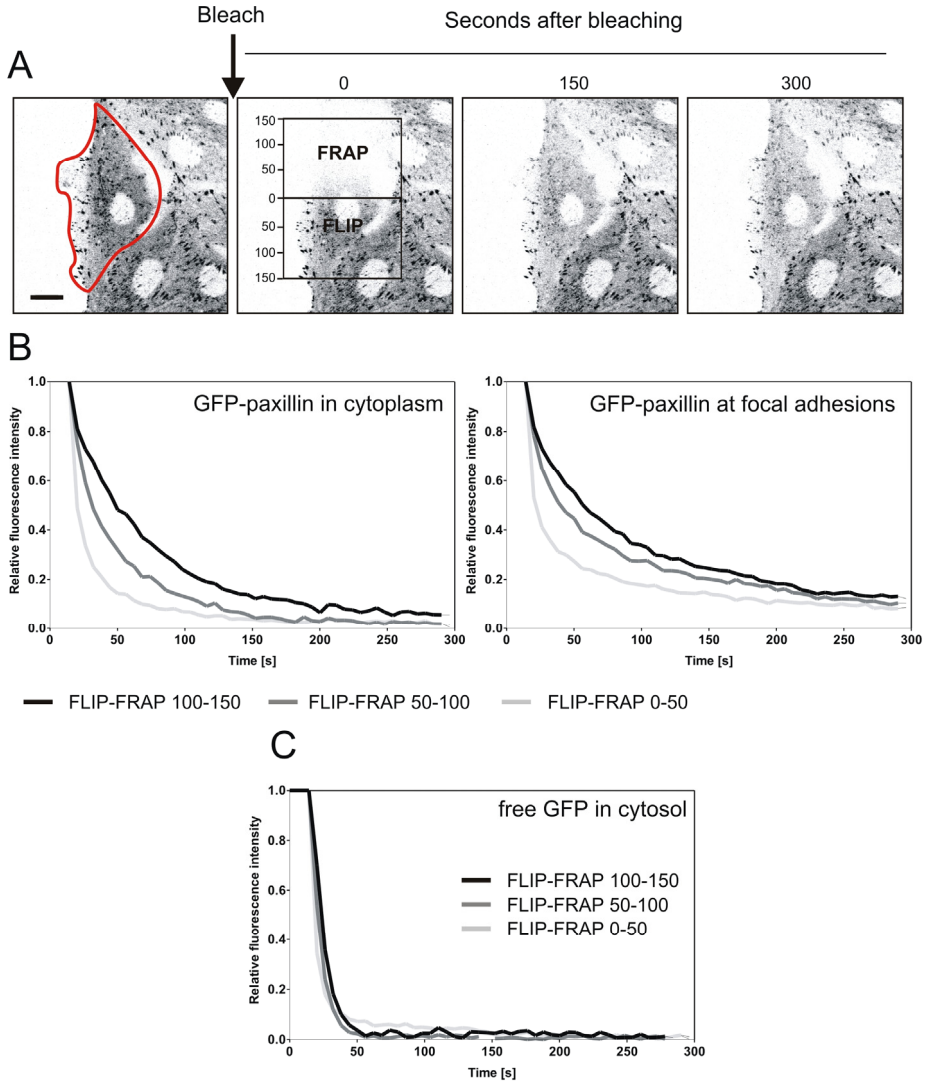


Figure S4: Simultaneous FLIP-FRAP (=half-FRAP) of focal-adhesion bound GFP-paxillin. (A) FLIP-FRAP on living LLC-PK1 cells expressing GFP-paxillin. Cells are photobleached over a region covering about one half of the cell (indicated by black boxes). The images were acquired before bleaching and at 6-s intervals after bleaching. Scale bar is 10 μm . (B) FLIP-FRAP analysis of redistribution of GFP-paxillin in the cytoplasm and at focal adhesion (in the 3 different regions). (C) FLIP-FRAP analysis of redistribution of free GFP in the cytoplasm (in the 3 different regions).

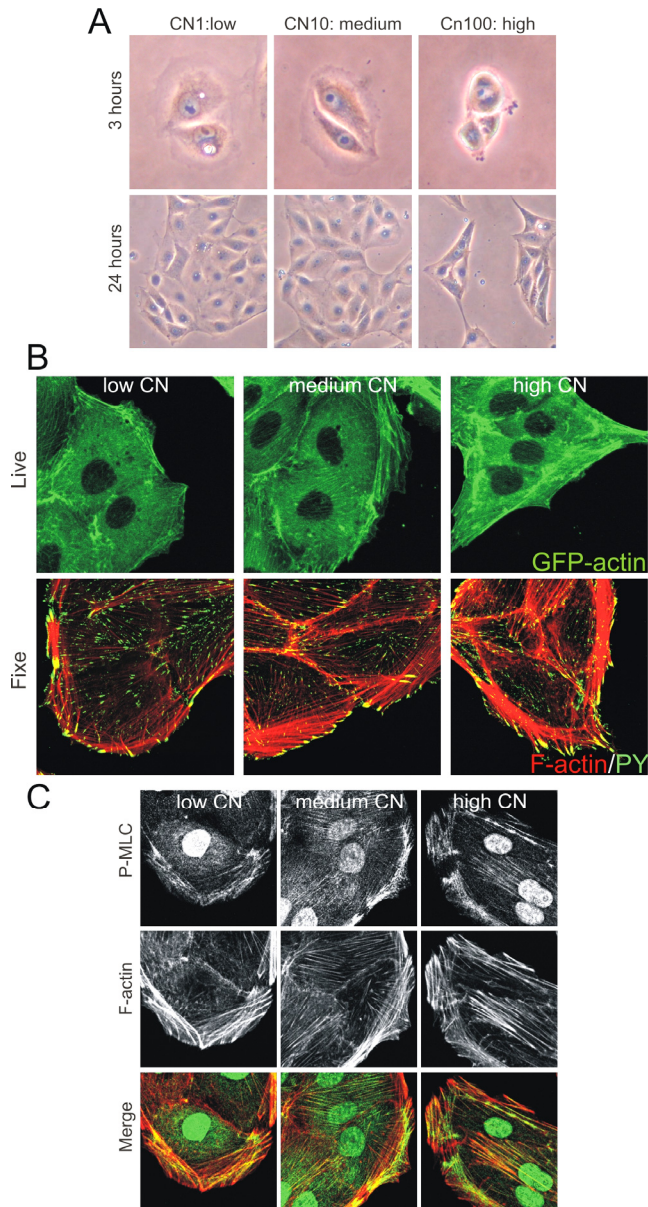


Figure S5: Adhesion strength affects cell spreading as well as F-actin and focal adhesion organization. (A) LLC-PK1 cells 3 hr and 24 h after plating on coverslips coated with the indicated CN concentration. (B) Live GFP-actin expressing cells plated on increasing CN concentration (first row pictures) and F-actin phalloidin staining and phosphor-tyrosine immunofluorescence in LLC-PK1 cells plated on low (1 $\mu\text{g}/\text{ml}$), medium (10 $\mu\text{g}/\text{ml}$) and high (100 $\mu\text{g}/\text{ml}$) CN. Merge: F-actin=red, PY=green. (C) F-actin phalloidin staining and serine 19-phosphorylated myosin regulatory light chain (pMLC) immunofluorescence in cells on low, medium and high CN. Merge: F-actin=red, P-MLC=green.

REFERENCE LIST

1. Mattern, K. A.; Swiggers, S. J.; Nigg, A. L. et al. Dynamics of protein binding to telomeres in living cells: implications for telomere structure and function. *Mol.Cell Biol.* 24: 5587-5594, 2004.
2. Zamir, E.; Geiger, B. Molecular complexity and dynamics of cell-matrix adhesions. *J.Cell Sci.* 114: 3583-3590, 2001.
3. Zaidel-Bar, R.; Cohen, M.; Addadi, L.; Geiger, B. Hierarchical assembly of cell-matrix adhesion complexes. *Biochem.Soc.Trans.* 32: 416-420, 2004.
4. Webb, D. J.; Parsons, J. T.; Horwitz, A. F. Adhesion assembly, disassembly and turnover in migrating cells -- over and over and over again. *Nat.Cell Biol.* 4: E97-100, 2002.
5. Webb, D. J.; Brown, C. M.; Horwitz, A. F. Illuminating adhesion complexes in migrating cells: moving toward a bright future. *Curr.Opin.Cell Biol.* 15: 614-620, 2003.
6. Berrier, A. L.; Yamada, K. M. Cell-matrix adhesion. *J Cell Physiol.* 213: 565-573, 2007.
7. Zamir, E.; Geiger, B. Molecular complexity and dynamics of cell-matrix adhesions. *J.Cell Sci.* 114: 3583-3590, 2001.
8. Webb, D. J.; Parsons, J. T.; Horwitz, A. F. Adhesion assembly, disassembly and turnover in migrating cells -- over and over and over again. *Nat.Cell Biol.* 4: E97-100, 2002.
9. Webb, D. J.; Brown, C. M.; Horwitz, A. F. Illuminating adhesion complexes in migrating cells: moving toward a bright future. *Curr.Opin.Cell Biol.* 15: 614-620, 2003.
10. Zaidel-Bar, R.; Cohen, M.; Addadi, L.; Geiger, B. Hierarchical assembly of cell-matrix adhesion complexes. *Biochem.Soc.Trans.* 32: 416-420, 2004.
11. Webb, D. J.; Donais, K.; Whitmore, L. A. et al. FAK-Src signalling through paxillin, ERK and MLCK regulates adhesion disassembly. *Nat.Cell Biol.* 6: 154-161, 2004.
12. Zaidel-Bar, R.; Itzkovitz, S.; Ma'ayan, A.; Iyengar, R.; Geiger, B. Functional atlas of the integrin adesome. *Nat.Cell Biol.* 9: 858-867, 2007.
13. Schaller, M. D.; Hildebrand, J. D.; Shannon, J. D. et al. Autophosphorylation of the focal adhesion kinase, pp125FAK, directs SH2-dependent binding of pp60src. *Mol Cell Biol.* 14: 1680-1688, 1994.
14. Turner, C. E. Paxillin interactions. *J.Cell Sci.* 113 Pt 23: 4139-4140, 2000.
15. Turner, C. E. Paxillin and focal adhesion signalling. *Nat.Cell Biol.* 2: E231-E236, 2000.
16. Cooley, M. A.; Broome, J. M.; Ohngemach, C.; Romer, L. H.; Schaller, M. D. Paxillin binding is not the sole determinant of focal adhesion localization or dominant-negative activity of focal adhesion kinase/focal adhesion kinase-related nonkinase. *Mol Biol Cell.* 11: 3247-3263, 2000.
17. Deakin, N. O.; Turner, C. E. Paxillin comes of age. *J Cell Sci.* 121: 2435-2444, 2008.
18. Brown, C. M.; Hebert, B.; Kolin, D. L. et al. Probing the integrin-actin linkage using high-resolution protein velocity mapping. *J Cell Sci.* 119: 5204-5214, 2006.
19. Hu, K.; Ji, L.; Applegate, K. T.; Danuser, G.; Waterman-Storer, C. M. Differential transmission of actin motion within focal adhesions. *Science.* 315: 111-115, 2007.
20. Phair, R. D.; Misteli, T. Kinetic modelling approaches to in vivo imaging. *Nat.Rev.Mol.Cell Biol.* 2: 898-907, 2001.
21. Houtsmuller, A. B.; Vermeulen, W. Macromolecular dynamics in living cell nuclei revealed by fluorescence redistribution after photobleaching. *Histochem.Cell Biol.* 115: 13-21, 2001.
22. Edlund, M.; Lotano, M. A.; Otey, C. A. Dynamics of alpha-actinin in focal adhesions and stress fibers visualized with alpha-actinin-green fluorescent protein. *Cell Motil.Cytoskeleton.* 48: 190-200, 2001.
23. Tsuruta, D.; Gonzales, M.; Hopkinson, S. B. et al. Microfilament-dependent movement of the beta3 integrin subunit within focal contacts of endothelial cells. *FASEB J.* 16: 866-868, 2002.
24. Geuijen, C. A.; Sonnenberg, A. Dynamics of the alpha6beta4 integrin in keratinocytes. *Mol.Biol.Cell.* 13: 3845-3858, 2002.
25. von Wichert, G.; Haimovich, B.; Feng, G. S.; Sheetz, M. P. Force-dependent integrin-cytoskeleton linkage formation requires downregulation of focal complex dynamics by Shp2. *EMBO J.* 22: 5023-5035, 2003.

26. Destaing, O.; Saltel, F.; Geminard, J. C.; Jurdic, P.; Bard, F. Podosomes display actin turnover and dynamic self-organization in osteoclasts expressing actin-green fluorescent protein. *Mol.Biol.Cell.* 14: 407-416, 2003.
27. Giannone, G.; Ronde, P.; Gaire, M. et al. Calcium rises locally trigger focal adhesion disassembly and enhance residency of focal adhesion kinase at focal adhesions. *J.Biol.Chem.* 279: 28715-28723, 2004.
28. Cluzel, C.; Saltel, F.; Lussi, J. et al. The mechanisms and dynamics of (alpha)v(beta)3 integrin clustering in living cells. *J.Cell Biol.* 171: 383-392, 2005.
29. Lele, T. P.; Pendse, J.; Kumar, S. et al. Mechanical forces alter zyxin unbinding kinetics within focal adhesions of living cells. *J.Cell Physiol.* 207: 187-194, 2006.
30. Endlich, N.; Otey, C. A.; Kriz, W.; Endlich, K. Movement of stress fibers away from focal adhesions identifies focal adhesions as sites of stress fiber assembly in stationary cells. *Cell Motil.Cytoskeleton.* 64: 966-976, 2007.
31. Goetz, J. G.; Joshi, B.; Lajoie, P. et al. Concerted regulation of focal adhesion dynamics by galectin-3 and tyrosine-phosphorylated caveolin-1. *J Cell Biol.* 180: 1261-1275, 2008.
32. Wolfenson, H.; Lubelski, A.; Regev, T. et al. A role for the juxtamembrane cytoplasm in the molecular dynamics of focal adhesions. *PLoS.ONE.* 4: e4304-2009.
33. van de, W. B.; Houtepen, F.; Huigsloot, M.; Tijdens, I. B. Suppression of chemically induced apoptosis but not necrosis of renal proximal tubular epithelial (LLC-PK1) cells by focal adhesion kinase (FAK). Role of FAK in maintaining focal adhesion organization after acute renal cell injury. *J.Biol.Chem.* 276: 36183-36193, 2001.
34. Essers, J.; Houtsmuller, A. B.; van Veelen, L. et al. Nuclear dynamics of RAD52 group homologous recombination proteins in response to DNA damage. *EMBO J.* 21: 2030-2037, 2002.
35. Farla, P.; Hersmus, R.; Trapman, J.; Houtsmuller, A. B. Antiandrogens prevent stable DNA-binding of the androgen receptor. *J Cell Sci.* 118: 4187-4198, 2005.
36. Farla, P.; Hersmus, R.; Geverts, B. et al. The androgen receptor ligand-binding domain stabilizes DNA binding in living cells. *J.Struct.Biol.* 147: 50-61, 2004.
37. Katz, B. Z.; Zamir, E.; Bershadsky, A. et al. Physical state of the extracellular matrix regulates the structure and molecular composition of cell-matrix adhesions. *Mol.Biol.Cell.* 11: 1047-1060, 2000.
38. Zamir, E.; Katz, B. Z.; Aota, S. et al. Molecular diversity of cell-matrix adhesions. *J.Cell Sci.* 112 (Pt 11): 1655-1669, 1999.
39. Li, S.; Guan, J. L.; Chien, S. Biochemistry and biomechanics of cell motility. *Annu.Rev Biomed Eng.* 7: 105-150, 2005.
40. Adelstein, R. S.; Conti, M. A. Phosphorylation of platelet myosin increases actin-activated myosin ATPase activity. *Nature.* 256: 597-598, 1975.
41. Gupton, S. L.; Waterman-Storer, C. M. Spatiotemporal feedback between actomyosin and focal-adhesion systems optimizes rapid cell migration. *Cell.* 125: 1361-1374, 2006.
42. Hamadi, A.; Bouali, M.; Dontenwill, M. et al. Regulation of focal adhesion dynamics and disassembly by phosphorylation of FAK at tyrosine 397. *J.Cell Sci.* 118: 4415-4425, 2005.
43. Lele, T. P.; Thodeti, C. K.; Ingber, D. E. Force meets chemistry: analysis of mechanochemical conversion in focal adhesions using fluorescence redistribution after photobleaching. *J.Cell Biochem.* 97: 1175-1183, 2006.
44. Lele, T. P.; Thodeti, C. K.; Pendse, J.; Ingber, D. E. Investigating complexity of protein-protein interactions in focal adhesions. *Biochem.Biophys.Res.Commun.* 369: 929-934, 2008.
45. Digman, M. A.; Brown, C. M.; Sengupta, P. et al. Measuring fast dynamics in solutions and cells with a laser scanning microscope. *Biophys.J.* 89: 1317-1327, 2005.
46. Balaban, N. Q.; Schwarz, U. S.; Riveline, D. et al. Force and focal adhesion assembly: a close relationship studied using elastic micropatterned substrates. *Nat Cell Biol.* 3: 466-472, 2001.
47. Goffin, J. M.; Pittet, P.; Csucs, G. et al. Focal adhesion size controls tension-dependent recruitment of alpha-smooth muscle actin to stress fibers. *J.Cell Biol.* 172: 259-268, 2006.
48. Yoshigi, M.; Hoffman, L. M.; Jensen, C. C.; Yost, H. J.; Beckerle, M. C. Mechanical force mobilizes zyxin from focal adhesions to actin filaments and regulates cytoskeletal reinforcement. *J Cell Biol.* 171: 209-215, 2005.

49. Zaidel-Bar, R.; Milo, R.; Kam, Z.; Geiger, B. A paxillin tyrosine phosphorylation switch regulates the assembly and form of cell-matrix adhesions. *J Cell Sci.* 120: 137-148, 2007.

